Parity-dependent oscillations in collisional polarization transfer: CN(A 2, v = 4) + Ar

S. J. McGurk, K. G. McKendrick, M. L. Costen, M. H. Alexander, and P. J. Dagdigian

Citation: The Journal of Chemical Physics **139**, 124304 (2013); doi: 10.1063/1.4821602

View online: http://dx.doi.org/10.1063/1.4821602

View Table of Contents: http://scitation.aip.org/content/aip/journal/jcp/139/12?ver=pdfcov

Published by the AIP Publishing

Parity-dependent oscillations in collisional polarization transfer: CN($A^2\Pi$, v = 4) + Ar

S. J. McGurk,[1] K. G. McKendrick,[1] M. L. Costen,[1,a)] M. H. Alexander,[2] and P. J. Dagdigian[3,b)]

[1]*School of Engineering and Physical Sciences, Heriot-Watt University, Edinburgh EH14 4AS, United Kingdom*
[2]*Department of Chemistry and Biochemistry and Institute for Physical Science and Technology, University of Maryland, College Park, Maryland 20742-2021, USA*
[3]*Department of Chemistry, The Johns Hopkins University, Baltimore, Maryland 21218-2685, USA*

(Received 11 July 2013; accepted 3 September 2013; published online 25 September 2013)

We report the first systematic experimental and theoretical study of the state-to-state transfer of rotational angular momentum orientation in a $^2\Pi$-rare gas system. CN($X^2\Sigma^+$) was produced by pulsed 266 nm photolysis of ICN in a thermal bath (296 K) of Ar collider gas. A pulsed circularly polarized tunable dye laser prepared CN($A^2\Pi$, v = 4) in two fully state-selected initial levels, $j = 6.5$ F_1e and $j = 10.5$ F_2f, with a known laboratory-frame orientation. Both the prepared levels and a range of product levels, j' F_1e and j' F_2f, were monitored using the circular polarized output of a tunable diode laser *via* cw frequency-modulated (FM) spectroscopy in stimulated emission on the CN(*A*-*X*) (4,2) band. The FM Doppler lineshapes for co-rotating and counter-rotating pump-and-probe geometries reveal the time-dependence of the populations and orientations. Kinetic fitting was used to extract the state-to-state population transfer rate constants and orientation multipole transfer efficiencies (MTEs), which quantify the degree of conservation of initially prepared orientation in the product level. Complementary full quantum scattering (QS) calculations were carried out on recently computed *ab initio* potential energy surfaces. Collision-energy-dependent tensor cross sections for ranks $K = 0$ and 1 were computed for transitions from both initial levels to all final levels. These quantities were integrated over the thermal collision energy distribution to yield predictions of the experimentally observed state-to-state population transfer rate constants and MTEs. Excellent agreement between experiment and theory is observed for both measured quantities. Dramatic oscillations in the MTEs are observed, up to and including changes in the sign of the orientation, as a function of even/odd Δj within a particular spin-orbit and *e*/*f* manifold. These oscillations, along with those also observed in the state-to-state rate constants, reflect the rotational parity of the final level. In general, parity-conserving collisions conserve rotational orientation, while parity-changing collisions result in large changes in the orientation. The QS calculations show that the dynamics of the collisions leading to these different outcomes are fundamentally different. We propose that the origin of this behavior lies in interferences between collisions that sample the even and odd-λ terms in the angular expansions of the PESs. © *2013 AIP Publishing LLC*. [http://dx.doi.org/10.1063/1.4821602]

I. INTRODUCTION

Collision induced rotational energy transfer (RET) is a ubiquitous process in any gas-phase environment, and understanding this phenomenon is fundamental to the modeling of a wide range of technological and natural environments.[1] Particular interest has been paid to collisions of small open-shell species, which are often found in combustion, plasma, atmospheric, or astrochemical systems, such as OH, NO, or the subject of this study, CN. These radicals are particularly suitable for study, as they are amenable to experiment, being relatively easily produced and having well known and accessible spectroscopy. Crucially, they are also small enough that their collisions with rare gases may be the subject of quantum scattering (QS) calculations on accurate *ab initio* potential energy surfaces (PESs). They have therefore been the subject of many comparisons of experiment and theory, providing fundamental tests of the development of scattering theory and of the PESs that underpin the scattering calculations.

Experimental measurements that explore the vector properties of a collision have been shown to be more sensitive probes of the scattering dynamics than simple scalar measurements of product rotational levels.[2] Molecular beam based methods have been extensively applied to study collisions of the stable radical NO($X^2\Pi$) with rare gas colliders, particularly He and Ar.[3–8] These experiments can provide high resolution differential scattering cross sections (DCS) with full rotational and fine-structure state resolution, together with the scattering angle dependence of the product rotational angular momentum polarization,[4,5] and experiment and theory now have essentially quantitative agreement for these systems.

Experiments using molecular beam methods to study reactive or electronically excited radicals are substantially more

a)Electronic mail: m.l.costen@hw.ac.uk
b)Electronic mail: pjdagdigian@jhu.edu

challenging, but recently NO($A^2\Sigma^+$) + Ar/He[9–11] DCS measurements have been reported, together with associated QS calculations. The OH($X^2\Pi$) + Ar system has also been studied in elegant experiments applying hexapole state-selection and a quadrupole electric field to orient the OH bond-axis relative to the rare gas beam. Cross sections for the elastic ($\Delta j = 0$) reorientation of the OH angular momentum were determined, displaying a strong propensity for conservation of initial state.[12] State-to-state DCSs in a conventional crossed-beam apparatus have also recently been reported for OH($X^2\Pi$) + He/Ar.[13] One substantial limitation of these crossed-beam methods is that the collision energy is generally substantially greater than the attractive well depth, so that the measured dynamics is dominated by the repulsive wall of the PES. While experimental advances, such as Stark deceleration,[14,15] may offer a means to reduce the collision energy, other experimental approaches can provide the means to access vector properties of collisions in the thermal energy range.

Another widely used experimental approach is optical-optical double resonance (OODR) in a thermal bath of the collider gas. A single rotational level of an excited state (vibrational, or more commonly electronic) is prepared by optical pumping. The collisional evolution of this prepared level or of product levels is then observed by spectroscopy. This is a standard approach used to measure rotational level specific removal rate constants, or level-to-level population transfer rate constants.[1,16] Polarized laser excitation will also result in a prepared population with a laboratory-frame polarization of the rotational angular momentum. This can be either oriented or aligned, depending on the pump laser polarization. Polarization resolution in the probe step then enables the measurement of the collisional evolution of this orientation or alignment, either as depolarization of the initial rotational level, or transfer of population to product levels with some retention of polarization.

The different experimental approaches to the measurement of this $\boldsymbol{j}.\boldsymbol{j}'$ vector correlation have been discussed by us in a recent review article,[17] which also summarizes the rigorous relationships between experimental observables and scattering calculations that have recently been derived.[18–20] Our previous experiments in this area have focused on collisional depolarization of the initially prepared level, usually termed "elastic depolarization". This has included using the third-order nonlinear Polarization Spectroscopy technique to study depolarization in OH($X^2\Pi$) + He/Ar/Xe,[21–23] OH($X^2\Pi$) + N_2/O_2,[24] OH($A^2\Sigma^+$) + He/Ar,[25] and NO($X^2\Pi$) + Ar.[26] We have also applied OODR with ns pulsed excitation and cw probe to study the elastic depolarization in CN($A^2\Pi$) + Ar.[27,28] In the initial measurements of the collisional removal of alignment the Edinburgh authors observed rapid depolarization of the initial levels.[28]

Subsequently, more extensive measurements that included collisional removal of orientation in Edinburgh, and QS calculations on new *ab initio* PESs of the population and polarization removal by the US authors, demonstrated that this was not elastic depolarization.[27] Although the collisional depolarization of the orientation and alignment of the initially prepared level is generally rapid, and is reproduced by master equation modeling using the QS results, it was shown clearly to be the result of multiple *inelastic* collisions. In this paper we report the extension of this technique to study product-level resolved *transfer* of orientation in single collisions of CN(A) + Ar, and compare the experimental results to QS calculations on the recently introduced PESs. To the best of our knowledge, this is the first systematic initial and final level resolved experimental and theoretical study of inelastic polarization transfer in an open-shell species, and in particular in an electronic state possessing non-zero orbital angular momentum.

There have been a significant number of studies of polarization transfer using OODR techniques since the first experiments on the inelastic transfer of polarization were performed by McCaffery and co-workers in the 1970s.[29–32] Many of the studies have been on electronic states of singlet spin multiplicity, for example, $Li_2(A^1\Sigma_u^+)$,[32] BaO($A^1\Sigma^+$),[33] $N_2(X^1\Sigma_g^+)$,[34] $C_2H_2(X^1\Sigma_g^+)$,[35] NaK($A^1\Sigma^+$),[36] and $H_2CO(\tilde{A}^1A_2)$.[37,38] Although some early work suggested that the laboratory-frame polarization was strongly conserved in inelastic collisions, in general this is not the case. In collisions between singlet states and inert gas partners, the polarization is observed to be conserved along the kinematic apse, $\boldsymbol{a} = (\boldsymbol{k}' - \boldsymbol{k})/(|\boldsymbol{k}' - \boldsymbol{k}|)$, consistent with a rigid or hard-shell collision.[39] When scattering is strongly in the forward direction, likely for small Δj transfer, the apse direction will lie close to $\boldsymbol{k}$ and $\boldsymbol{k}'$. Conservation in the apse-frame then corresponds to conservation in the collision-frame, and since the $\boldsymbol{k}.\boldsymbol{k}'$ angle is small this results in strong laboratory-frame conservation. In contrast, when scattering is across a wider range of $\boldsymbol{k}.\boldsymbol{k}'$ angles in the sideways and backwards directions, for example, for large Δj transfer, the kinematic apse typically lies at a wide range of angles to $\boldsymbol{k}$. In this case, conservation in the apse-frame no longer results in strong conservation in the laboratory-frame, although some laboratory-frame product polarization is usually observed. Only when a strongly attractive potential is present, for example, when the collision partner is reactive, as in the NaK($A^1\Sigma^+$) + K exchange process, is essentially complete depolarization observed.[36]

Collisions of open-shell systems present additional complexity to the scattering problem, with the possibility of a strong dependence of the scattering on the fine structure of the initial and final levels. The simplest example of this is with spin-rotation (SR) coupling in Σ electronic states with non-zero total electron spin **S**. As first shown by Alexander and Davis,[40] the electron spin is a spectator to the collision, which reorients the rotational angular momentum of the nuclear motion, **N**. The spin **S** subsequently recouples to **N** after collision to form the fine-structure levels. The direction in space of **S** does not change in the collision, and hence for a collision to cause a change in fine-structure state it must change the direction of **N**. Collisions that cause substantial reorientation of **N** therefore also result in SR transfer. This effect has been observed by Brouard and co-workers in their recent series of experiments and associated scattering calculations on the OH($A^2\Sigma^+$) + Ar/Kr and NO($A^2\Sigma^+$) + He/Ar systems.[20,25,41–45]

Non-zero electronic orbital angular momentum introduces the additional complexity of both spin-orbit and Λ-doublet fine structure splittings. For a $^2\Pi$ electronic state, the spin-orbit levels, with body-frame projection of the angular momentum $\Omega = 1/2$ or 3/2, are labeled F_1 and F_2, with F_1 lower in energy. In each spin-orbit manifold, the rotational levels appear in nearly-degenerate pairs, called Λ-doublets. The parity p of these Λ-doublets depends on the rotational angular momentum j and the symmetry index[46] ε of the Λ-doublet, with $p = \varepsilon(-1)^{j-1/2}$. The Λ-doublets with $\varepsilon = +1$ are given the spectroscopic label e, while those with $\varepsilon = -1$ are labeled as f.[47] Hence, within a particular Λ-doublet manifold the total parity p alternates as a function of j, while e/f Λ-doublet pairs with the same j have the opposite parity.

The approach of a rare gas atom toward a molecule in a $^2\Pi$ electronic state results in two separate adiabatic PESs, of A' and A'' symmetry with respect to reflection in the triatomic plane. QS calculations are most conveniently performed in a diabatic basis,[46,48] with $V_{\rm sum}$ and $V_{\rm dif}$ PESs defined as

$$V_{\rm sum}(R,\theta) = \frac{1}{2}\left[V_{A''}(R,\theta) + V_{A'}(R,\theta)\right], \tag{1a}$$

$$V_{\rm dif}(R,\theta) = \frac{1}{2}\left[V_{A''}(R,\theta) - V_{A'}(R,\theta)\right], \tag{1b}$$

where R is the atom-molecule separation and θ is the angle between **R** and the diatomic axis **r**. In the Hund's case (a) coupling limit, scattering within a single spin-orbit manifold is controlled by the $V_{\rm sum}$ PES, while the $V_{\rm dif}$ PES controls scattering between different spin-orbit manifolds. In the majority of systems, and particularly as j increases, the case (a) limit will no longer apply, and both the $V_{\rm sum}$ and $V_{\rm dif}$ PESs will contribute to the scattering within and between spin-orbit manifolds.[49] A significant result of this analysis is the derivation of rotational parity propensity rules for inelastic scattering in $^2\Pi$ + Rg (Rg = rare gas) systems. This is seen most clearly if the PESs are expanded in reduced rotation matrix elements[46]

$$V_{\rm sum}(R,\theta) = \sum_{\lambda=0}^{\lambda_{\rm max}} V_{\lambda 0}(R)\, d^{\lambda}_{00}(\theta), \tag{2a}$$

$$V_{\rm dif}(R,\theta) = \sum_{\lambda=2}^{\lambda_{\rm max}} V_{\lambda 2}(R)\, d^{\lambda}_{20}(\theta), \tag{2b}$$

which defines the radial expansion coefficients $V_{\lambda 0}(R)$ and $V_{\lambda 2}(R)$. It is then found that the scattering amplitude for rotational parity-*conserving* transitions arises from only the *even*-λ terms of the expansions, while the parity-*changing* collisions result from the *odd*-λ terms.[48,49] The even and odd terms of the angular expansions often have very different dependences on R, which gives rise to a strong parity dependence of the population transfer cross sections in $^2\Pi$ + Rg collisions, first seen experimentally for CaF($A^2\Pi$) + Ar and He by Dufour *et al.*[50]

Polarization transfer in $^2\Pi$ + Rg collisions was first considered by Alexander and Orlikowski for the NO($X^2\Pi$) + Ar system.[51] This work introduced the multipole transfer efficiency (MTE) as a measure of the polarization transferred and rigorously showed how these MTEs could be calculated in QS calculations. The MTE, $E^{(K)}(j, j')$, can be defined in terms of the ratio of the cross section for transfer of a moment of rank K of the angular momentum distribution, $\sigma^{(K)}_{j\to j'}$, to the population transfer tensor cross section, $\sigma^{(0)}_{j\to j'}$ (or the equivalent ratio for rates or rate constants):[17,19,20]

$$E^{(K)}(j, j') = \frac{\sigma^{(K)}_{j\to j'}}{\sigma^{(0)}_{j\to j'}}. \tag{3}$$

The MTE for the lowest orientation moment, $K = 1$, has the limits $-1 \le E^{(K=1)}(j, j') \le +1$, where the positive limit corresponds to complete conservation of the initial orientation and the negative limit corresponds to conservation of the magnitude, but change in the *sign* of orientation. Alexander and Orlikowski found a strong Λ-doublet dependence to the orientation MTE, involving either conservation or change in the sign of the *laboratory-frame* orientation. However, despite this surprising prediction, no experiments have been performed to date to test this on the NO(X) + Ar system.

To the best of our knowledge, the only prior experimental measurements of MTE for collisions of a $^2\Pi$ system, other than our own,[28] are those of Field and co-workers on the CaF($A^2\Pi$) + Ar system.[52] In these OODR experiments, they prepared CaF purely in the $A^2\Pi_{1/2}$ $j = 0.5f$, $m = +0.5$ level by cw laser circularly polarized pump excitation, and then probed the $A^2\Pi_{1/2}$ $j' = 0.5e$, $1.5f$, and $1.5e$ product levels with left and right polarized cw LIF. They observed a strong final level dependence of the product orientation, with the parity-conserving transfer ($j' = 1.5f$) resulting in products with the same sign of orientation as the initial level, while the parity-changing transfer ($j' = 0.5e$ and $1.5e$) resulted in products with the opposite sign of orientation. This corresponds to a positive MTE for the parity-conserving collisions and a negative MTE for the parity-changing collisions, exactly as predicted earlier by Alexander and Davis,[53] and clearly related to the behavior observed in the NO($X^2\Pi$) + Ar system by Alexander and Orlikowski.[51]

The CN($A^2\Pi$) + Ar system has been the subject of multiple previous studies of state-to-state population transfer by both experiment and QS calculations. In particular, Dagdigian, Alexander, and Yang have performed systematic experiments and calculations measuring transfer at a fully state-resolved ($jF\varepsilon \to j'F'\varepsilon'$) level for the v = 3 level both near the peak of the rotational distribution ($j = 6.5$) and at very high j ($N = 60$).[54–56] The Edinburgh authors have previously published some limited measurements of state-to-state population transfer in the v = 4 level using the technique applied in the work presented here, along with the only previous measurements of polarization transfer, in that case of alignment, in CN(A) + Ar.[28] In all of these studies of population transfer, rotational parity-dependent effects were observed in the state-to-state rate constants, as predicted by the propensity rules.[48] In this work, we present a systematic experimental and theoretical study of the fully state-resolved transfer of population and orientation from two initial levels, $j = 6.5$ F_1e and $j = 10.5$ F_2f, to a wide range of rotational product levels in both spin-orbit conserving and changing transitions, which cover both parity-conserving and parity-changing transitions in each case.

II. METHODOLOGY

A. Experimental

The experimental apparatus has been described in detail previously.[27,28,57–59] The experiments were performed in a 2 m long longitudinal vacuum chamber, within a region shielded by a μ-metal cylinder to isolate the sample from stray magnetic fields.[60] A mixture of ICN ($\leq$5 mTorr) and Ar (research grade, BOC) was flowed slowly through the chamber, with the total pressure maintained at either 400 $\pm$ 5 mTorr ($j = 10.5\ F_2f$) or 440 $\pm$ 5 mTorr ($j = 6.5\ F_1e$). The ICN was photolyzed at 266 nm using a Nd:YAG laser (Continuum Surelite III-10) to produce CN($X^2\Sigma^+$, v = 0). A post-photolysis delay of 30 μs ensured thermalization of the nascent translational and rotational distributions, and that the strong rotational alignment of CN(X) produced in this photolysis[59,61] was destroyed.

The strongly saturating output ($\approx$65 mJ cm^{-2}) of a Nd:YAG pumped dye laser (Spectron SL803/SL4000) was co-propagated along the photolysis beam, and tuned to either the $R_1(5.5)$ or $P_2(11.5)$ transition of the CN $A^2\Pi - X^2\Sigma^+$ (4,0) band, preparing an oriented sample of CN $A^2\Pi$(v = 4) $j = 6.5$ F_1e or $j = 10.5$ F_2f, respectively. The pump beam polarization was switched between left- and right-handed circular by a photo-elastic modulator (PEM-80, Hinds Inc.) immediately before the vacuum chamber. The timing of the photolysis and pump laser pulses relative to the PEM compression cycle was controlled by a digital delay generator (SRS DG535), under experimental software control.

Both the initially prepared and RET final ($|\Delta j| \leq \pm 5$) CN($A^2\Pi$, v = 4, $jF\varepsilon$) levels were probed by frequency-modulated (FM) stimulated emission using an external cavity tunable diode laser (Sacher GmbH, TEC520) on selected R_1, P_2, and $R_2 + {}^PQ_{21}$ rotational transitions of the $A^2\Pi$–$X^2\Sigma^+$ (4,2) band between 827 and 835 nm. Note that although the probe is in *stimulated emission*, we have retained the nomenclature of absorption here, for consistency with the spectroscopy in the pump step. The circularly polarized FM probe beam counter-propagated the photolysis and pump beams in a double-pass configuration, and was detected by a 1 GHz photo-receiver (New Focus, 1601FS-AC). The probe laser beam was step-scanned across the transition of interest in 100 MHz increments, and the transient in-phase (I) and quadrature (Q) signals were independently averaged (20–50 laser shots) using a digital storage oscilloscope (LeCroy LT342). A scanning Fabry-Perot interferometer (CVI Technical Optics, free spectral range 2 GHz) was used to monitor the modulated diode beam, and the recorded output was subsequently used to linearize the frequency scale of the spectra.

At each wavelength step the pump laser polarization was switched between left- and right-handed circular, giving two experimental geometries that we refer to as *co-rotating* (co) and *counter-rotating* (con), respectively. The photolysis of ICN at 266 nm produces a small fraction of CN $X^2\Sigma^+$ in v = 2,[62] resulting in a background absorption signal. Additional I&Q transient signals were therefore acquired at each wavelength step and for each polarization in the absence of the pump pulse. Hence, at each probe wavelength step, four sets of I&Q transient signals were acquired sequentially: pump-induced signal and background for the first geometry; followed by pump-induced signal and background for the second geometry. To minimize systematic errors arising from slow drifts in the pump laser wavelength, spectra were acquired alternately for the *prepared* and the *product* states.

B. Quantum scattering calculations

With QS calculations we have determined energy dependent state-to-state tensor cross sections for collisions of CN($X^2\Pi$) with Ar. The PESs used is described in our previous study of CN($X^2\Pi$)–Ar collisional depolarization.[27] Close-coupling calculations were carried out with the HIBRIDON suite of programs,[63] which was recently extended to include calculation of tensor cross sections for open-shell molecules.[18] The state-to-state tensor cross section of rank K for a molecule in a $^2\Pi$ electronic state is given by[18,32,40]

$$\sigma^{(K)}_{jF\varepsilon\rightarrow j'F'\varepsilon'} = \frac{\pi}{k^2_{jF\varepsilon}} \sum_{\substack{JJ'\\ ll'}} [J][J'](-1)^{l+l'-j-j'+2J} \begin{Bmatrix} j & j & K \\ J & J' & l \end{Bmatrix} \times \begin{Bmatrix} j & j & K \\ J & J' & l' \end{Bmatrix} T^J_{jF\varepsilon l, j'F'\varepsilon' l'} \left(T^{J'}_{jF\varepsilon l, j'F'\varepsilon' l'}\right)^*, \tag{4}$$

where $k_{jF\varepsilon}$ is the wavevector of the initial level, J is the total angular momentum, l is the orbital angular momentum, $[x] = 2x + 1$, the term in curly brackets is a 6j symbol,[64] and the T are T-matrix elements, expressed in the space-fixed frame. It should be noted that the $K = 0$ tensor cross sections are related to the familiar integral cross sections in the following way:[18]

$$\sigma_{j\rightarrow j'} = ([j'] / [j])^{1/2} \sigma^{(0)}_{j\rightarrow j'}. \tag{5}$$

In the scattering calculations, care was taken to include a sufficient number of both energetically closed channels and partial waves to ensure convergence of the cross sections. At the highest energies considered (2000 cm^{-1}), the rotational basis included all levels with $j \leq 25.5$, and the scattering calculations included all total angular momenta $J \leq 400.5\ \hbar$. For the calculation of thermal rate constants, the cross sections were computed over a grid of collision energies, up to total energies of 2000 cm^{-1} and averaged over a room-temperature ($T = 298$ K) Maxwellian distribution of relative velocities.[65]

III. RESULTS

A. Experimental results

The one-photon linear FM probe method is only sensitive to moments of rank $K = 0$, 1, and 2,[66] and in an isotropic collision environment moments of different rank evolve independently as a function of time.[67] Optical excitation imposes cylindrical symmetry upon the prepared distribution and the observed signal depends on population, $A^{(0)}_0$; orientation, $A^{(1)}_0$; and alignment, $A^{(2)}_0$, moments, of which the latter two have conventional high-j limits of -1 and $+1$, and -1 and $+2$, respectively.[68] The probe sensitivity to these moments

depends on both the spectroscopic branch used and the relative polarizations of the pump and probe lasers. The two geometries used in this work, *co* and *con*, have integral intensities, I_{co} and I_{con}, given in Eq. (6).

$$I_{(co)(con)} = \frac{ES}{3(2j+1)} A_0^{(0)} \left[1 - \frac{1}{2} h^{(2)}(j) A_0^{(2)} \pm \frac{3}{2} h^{(1)}(j) A_0^{(1)} \right], \tag{6}$$

where the (+) sign refers to I_{co} and the (−) sign refers to I_{con}. The experimental sensitivity to parameters such as optical path length, absolute number density, and detector response is contained in the parameter E, S is the rotational line strength factor, and $h^{(K)}(j)$ is the rotational branch sensitivity to the moment of rank K.[69,70]

There are three independent parameters in Eq. (6), of which two, $A_0^{(0)}$ and $A_0^{(2)}$, are detected with equal sensitivity in the two geometries used. The orientation we wish to determine appears as either an addition to, or a subtraction from, an overall intensity determined by $A_0^{(0)}$ and $A_0^{(2)}$. Time-dependent changes in the alignment term $A_0^{(2)}$, for example, from collisional alignment transfer, can thus result in apparent changes in the measured time-dependence of the orientation. This will only be a significant perturbation to the measured orientation if the alignment-dependent term contained within the square brackets in Eq. (6) is large relative to the population term within the brackets, i.e., is significant compared to unity. In our previous linear pump and probe measurements, as a result of the saturation of the pump step, the typical prepared alignment was $A_0^{(2)} \approx -0.3$.[27] Using circular pump polarization introduces an additional geometrical factor of −1/2, and $h^{(2)}(j) \approx -1/2$ for the P and R branches probed. The alignment contribution to the term in Eq. (6) contained in the square brackets is therefore

$$-\frac{1}{2} h^2(j) A_0^{(2)} \approx -\frac{1}{2}\left(-\frac{1}{2}\right)\left(-\frac{1}{2}\right)(-0.3) \approx +\frac{3}{80}. \tag{7}$$

Since this is small compared to unity, we have assumed in the analysis that follows that this alignment contribution to the overall intensity can be set to zero. Trial analysis of experimental data sets (using the procedure described in the following paragraph) with the alignment contribution fixed at the value given by Eq. (7) were also performed and were found to be consistent within experimental uncertainty to those in which this contribution was neglected.

The experimental data were analyzed as FM Doppler line shapes in custom-written LabVIEW® routines. The acquired FM background 2D arrays were first subtracted from the corresponding signal arrays for each experimental geometry. The background-subtracted I&Q arrays were then rotated to yield pure stimulated emission (SE) and dispersion (D) arrays.[71] FM Doppler line shapes for sequential 10 ns averages of the SE and D signals for each geometry were constructed, with the wavelength axis linearized using the acquired monitor etalon traces.

Gaussian Doppler profiles for the two geometries were simulated from assumed $A_0^{(0)}$ and $A_0^{(1)}$ moments with intensities given by Eq. (6). The simulated profiles were then transformed into FM SE and D line shapes and simultaneously least-squares fitted using the Levenberg-Marquardt (LM) method to the experimental FM line shapes, optimizing the $A_0^{(0)}$ and $A_0^{(1)}$ moments. For the initial levels, the translational temperature was also optimized. The temperature of these levels decreased from a slightly elevated initial temperature (≈330 K), typically by 40–50 K over the first 500 ns, as a consequence of the more rapid collisional removal-rate of the faster-moving CN within the Maxwell-Boltzmann distribution. At later times the initial level temperatures recovered to the room-temperature average, 296 K. The lower signal-to-noise ratio for the transferred levels resulted in unphysical and unstable oscillations in the fitted temperature for the 10 ns average profiles. Fitting of 100 ns averages resulted in best-fit temperatures consistent with the room-temperature of 296 K, and hence the transferred levels were subsequently fitted with the translational temperature fixed at this value. Representative data and fits for the stimulated emission FM line shapes are shown for the two initial levels and selected product levels in Fig. 1, where for the purposes of presentation the first 100 ns post-pump signal has been averaged. This Doppler profile analysis yielded the time dependence of the population and orientation, providing *kinetic* traces for subsequent fitting.

In our previous work,[27] we showed that the population and orientation or alignment of the initial level could be well described by a simple 3-level kinetic model. In principle, that model could be straightforwardly extended to describe the time dependence of the population and orientation of the product levels. However, in practice it was found that the observed signal to noise ratio of the product levels was not high enough to support such a model and the large number of associated parameters. We have therefore restricted our fitting to short delay times where the CN will have undergone one or a few collisions and have simplified the kinetic modelling accordingly.

Assuming that only a single collision has occurred, transferring molecules from j to j', the population of the product level at time, t, will be given by

$$A_0^{(0)}(j';t) = A_0^{(0)}(j;t=0)\left[\frac{\Gamma_{j\to j'}^{(0)}}{\Gamma_{j,\mathrm{tot}}^{(0)}}\right]\left(1 - e^{-\Gamma_{j,\mathrm{tot}}^{(0)} t}\right). \tag{8}$$

Here $A_0^{(0)}(j;t=0)$ is the population of the initial level at $t=0$, $\Gamma_{j,\mathrm{tot}}^{(0)}$ is the total population removal rate from the initial level and $\Gamma_{j\to j'}^{(0)}$ is the rate of population transfer from the initial level to the product level which we wish to find. We find the first two of these by fitting the kinetic trace for population of the *initial* level j to the three-level kinetic model discussed in our recent CN(A) + Ar depolarization paper.[27] This simple multiple collision model includes reversible transfer of population from j to nearby rotational levels j', described by the rates $\Gamma_{j\to j'}^{(0)}$ and $\Gamma_{j'\to j}^{(0)}$, and irreversible loss from both of these levels to distant levels, e.g., in energy, angular momentum, or even vibrational or electronic state, j_x, described by the rates $\Gamma_{j\to j_x}^{(0)} = \Gamma_{j'\to j_x}^{(0)}$. The (well determined) total removal rate $\Gamma_{j,\mathrm{tot}}^{(0)}$ is then the sum of $\Gamma_{j\to j'}^{(0)}$ and $\Gamma_{j\to j_x}^{(0)}$, while $A_0^{(0)}(j;t=0)$ is proportional to the overall signal size. Since the initial and product experimental scans were performed back-to-back

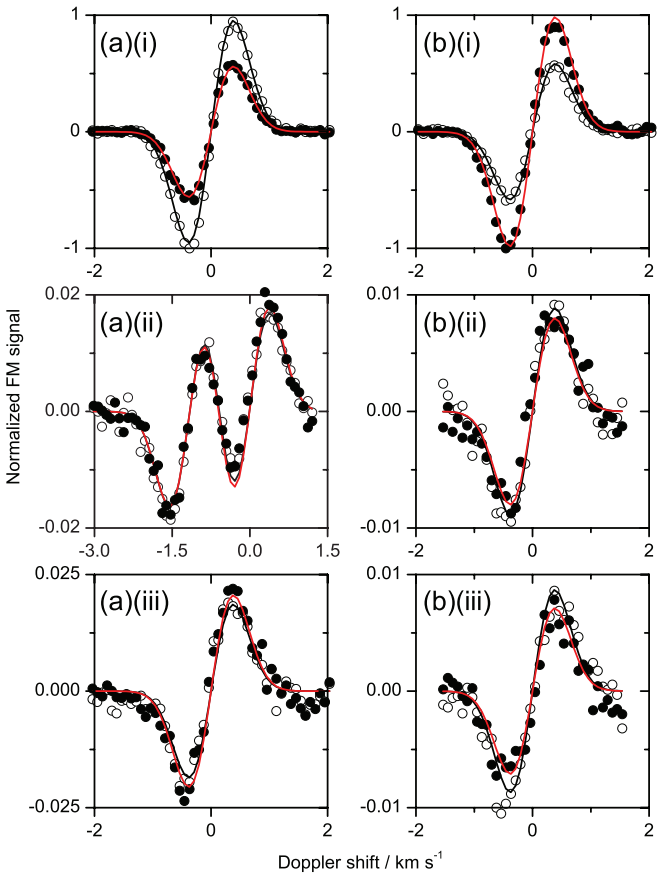

FIG. 1. Stimulated emission FM Doppler profiles for preparing (a) the $j = 6.5$ F_1e initial level on the $R_1(5.5)$ transition and (b) the $j = 10.5$ F_2f initial level on the $P_2(11.5)$ transition. For the $j = 6.5$ F_1e initial level, the probed final levels are (a)(i) the initial level probed on the $R_1(5.5)$ transition, (a)(ii) the $j = 6.5$ F_2f level ($\Delta j = 0$) probed on the $R_2(5.5) + {}^RQ_{21}(6.5)$ transition, and (a)(iii) the $j = 5.5$ F_2f level ($\Delta j = -1$) probed on the $P_2(6.5)$ transition. For the $j = 10.5$ F_2f initial level, the probed final levels are (b)(i) the initial level probed on the $P_2(11.5)$ transition, (b)(ii) the $j = 10.5$ F_1e level ($\Delta j = 0$) probed on the $R_1(9.5)$ line, and (b)(iii) the $j = 9.5$ F_1e level ($\Delta j = -1$) probed on the $R_1(8.5)$ transition. The final levels shown involve spin-orbit and Λ-doublet changing transitions. Each profile is a 100 ns average slice at early times (for clarity). Open points are *co*-rotating, filled points *counter*-rotating and the solid lines are fits to the data, as explained in the text.

under stable conditions, and the rotational line strengths were included in the data analysis to generate the kinetic traces, these proportionality constants are the same for the initial and final levels. We thus use $\Gamma^{(0)}_{j,\mathrm{tot}}$ and $A^{(0)}_0(j;t=0)$ in a fit to Eq. (8) to determine $\Gamma^{(0)}_{j\to j'}$, fitting to the first 200 ns of the product level population kinetic trace, which at the pressure used is the approximate average collision time, based on the observed total removal rates $\Gamma^{(0)}_{j,\mathrm{tot}}$.

The MTE that we seek to measure is defined as

$$E^{(1)}(j,j') = \frac{A^{(1)}_0(j';t=0)}{A^{(1)}_0(j;t=0)}, \tag{9}$$

which is simply the ratio of the product level to initial level orientation at time $t = 0$.[17,19,20,51] The orientation of the initial level at $t = 0$, $A^{(1)}_0(j;t=0)$, can be found by fitting the orientation kinetic trace for j to the 3-level model previously described for depolarization.[27] The orientation of the *product* level is, of course, ill-defined at $t = 0$, as at this time no population has been transferred. At early times when the majority of the CN has undergone either zero or one collision, e.g., in the first 100 ns, the orientation is still poorly determined. However, as population is transferred into the product level and the orientation gradually becomes better determined, it is simultaneously being reduced in magnitude as a result of multiple collisions. The problem is therefore to extrapolate the measured orientation at later times back to $t = 0$. The simplest model that could successfully fit the orientation kinetic traces was found to be a single exponential decay. We have therefore fitted the measured time-dependent transferred orientation to this form,

$$A^{(1)}_0(j';t) = A^{(1)}_0(j';t=0)e^{-\langle\Gamma^{(1)}_{\mathrm{dep}}\rangle t}, \tag{10}$$

by varying the phenomenological orientation depolarization rate, $\langle\Gamma^{(1)}_{\mathrm{dep}}\rangle$, and initial orientation, $A^{(1)}_0(j';t=0)$. The range of orientation data fitted was varied depending on the signal to noise, but was typically 100 ns $\le t \le$ 500 ns. We place no significance on the value of $\langle\Gamma^{(1)}_{\mathrm{dep}}\rangle$ and do not report or discuss it further.

In practice, these fitting procedures were performed by a single custom-written LabVIEW® routine. The population and orientation kinetic traces for an initial and product level that had been recorded in sequence without change to the experimental conditions were analyzed together, with the initial level population and orientation traces fitted to the 3-level model as outlined above. The obtained parameters: $\Gamma^{(0)}_{j,\mathrm{tot}}$, $A^{(0)}_0(j;t=0)$, and $A^{(1)}_0(j;t=0)$, were passed to subsequent algorithms that fitted the transferred population and orientation to find $\Gamma^{(0)}_{j\to j'}$, $A^{(1)}_0(j';t=0)$, and hence $E^{(1)}(j,j')$. In each case a LM minimization routine was used to perform the fitting, with weighting by statistical deviation of the data. Figure 2 shows representative data and fits for both initial levels and a pair of product levels; these are the kinetic traces arising from the raw spectra and fits shown in Fig. 1. In both Figs. 2(a) and 2(b) the orientation prepared in the initial level is significantly smaller in magnitude than the limiting value of ± 1, the result of the strong saturation of the pump step.[72] The transferred orientations are smaller in magnitude again, as is required by the limits of $E^{(1)}(j,j')$, and are clearly dependent on the final state. Strikingly, the orientation resulting from $\Delta j = 0$, spin-orbit and parity-changing transfer from $j = 6.5$ F_1e is of the opposite sign to that initially prepared, which we return to in the discussion below.

For each product rotational level, multiple independent measurements taken on different days were fitted separately. The resulting rates, $\Gamma^{(0)}_{j\to j'}$, were converted to state-to-state rate constants, $k^{(0)}_{j\to j'}$, assuming that the pressure of ICN was negligible, and hence that the total pressure measured represented the number density of the Ar collider, [Ar]:

$$\Gamma^{(0)}_{j\to j'} = k^{(0)}_{j\to j'}[\mathrm{Ar}]. \tag{11}$$

These independent multiple measurements of $k^{(0)}_{j\to j'}$, and the state-to-state MTEs, were then averaged. The results of this process are shown in Fig. 3 for transfer from the initial state $j = 6.5$ F_1e and in Fig. 4 for transfer from the initial state $j = 10.5$ F_2f, with 2σ standard errors from the independent multiple measurements.

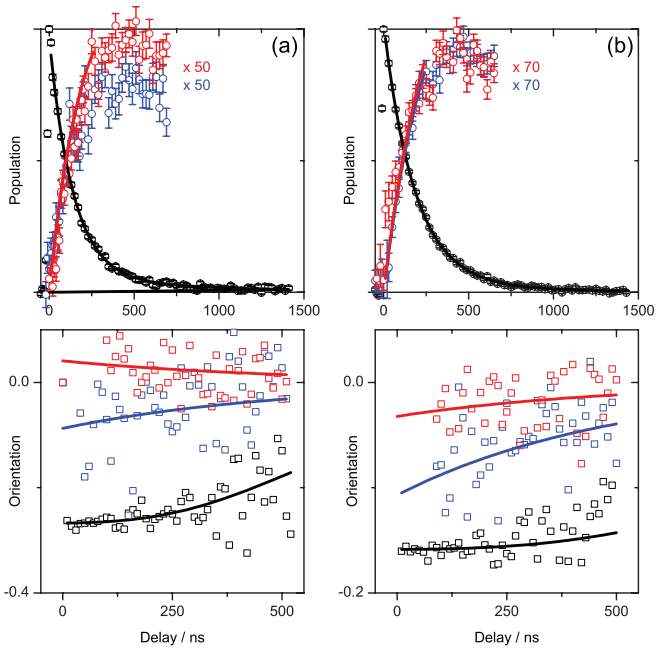

FIG. 2. Kinetic traces of the population (top panels), scaled as shown for the product levels, and orientation (lower panels) for preparing the (a) $j = 6.5$ F_1e and (b) $j = 10.5$ F_2f initial levels. The data points are 10 ns averages of the direct line (black), $\Delta j = 0$ (red), and $\Delta j = -1$ (blue) spin-orbit and Λ-doublet changing transitions, respectively. The solid lines are fits to the data according to the kinetic scheme outlined in the text, extrapolated to $t = 0$ ns for the product level orientation. Note that the fits to the transferred population traces are similar enough to be indistinguishable for these particular data sets.

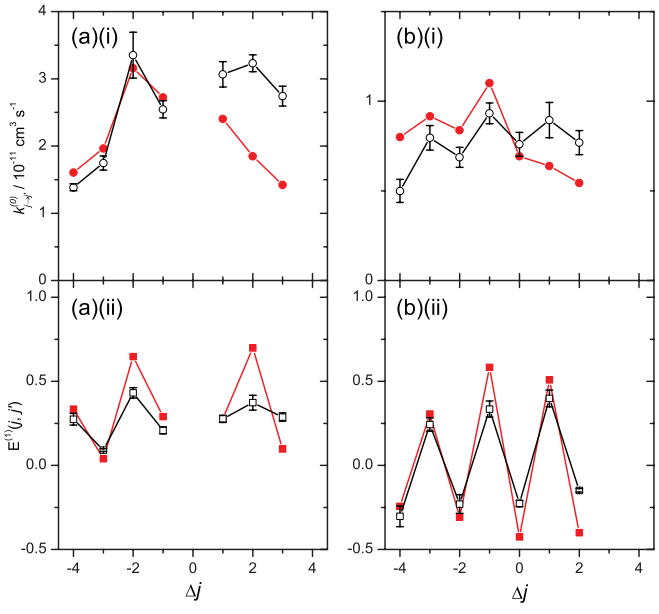

FIG. 3. (a)(i) and (b)(i) Bimolecular rate constants, $k^{(0)}_{j\to j'}$, for the transfer of population from the $j = 6.5$ F_1e level. (a) Spin-orbit and Λ-doublet conserving collisions to j' F_1e levels and (b) spin-orbit and Λ-doublet changing collisions to j' F_2f levels, as a function of $\Delta j = j' - j$. (a)(ii) and (b)(ii) The orientation multipole transfer efficiency, $E^{(1)}(j, j')$, for the same transitions. Open points are averages of 4–5 experimental measurements together with the 2σ standard error of the mean, filled points are from the QS calculations.

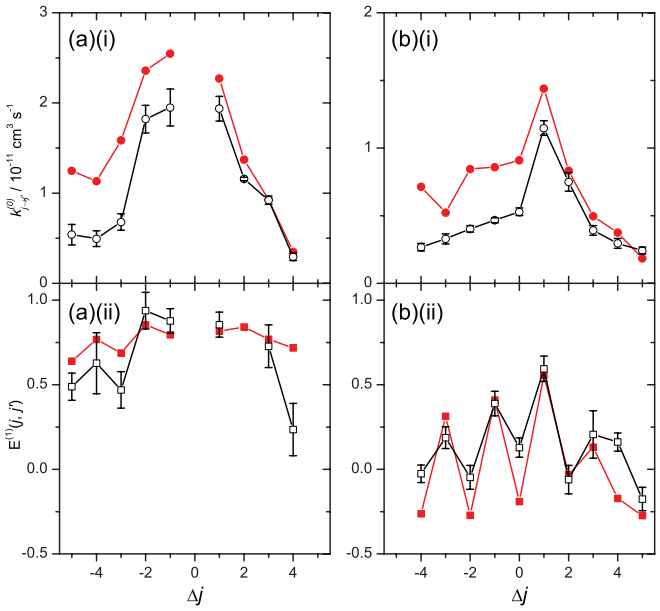

FIG. 4. (a)(i) and (b)(i) Bimolecular rate constants, $k^{(0)}_{j\to j'}$, for the transfer of population from the $j = 10.5$ F_2f level. (a) Spin-orbit and Λ-doublet conserving collisions to j' F_2f levels and (b) spin-orbit and Λ-doublet changing collisions to j' F_1e levels as a function of $\Delta j = j' - j$. (a)(ii) and (b)(ii) The orientation multipole transfer efficiency, $E^{(1)}(j, j')$, for the same transitions. Open points are averages of 4–5 experimental measurements together with the 2σ standard error of the mean, filled points are the results of the quantum scattering calculations.

B. QS calculations

Tensor cross sections for CN($A^2\Pi$,v = 4)–Ar collisions were computed for transitions out of the $j = 6.5$ F_1e and $j = 10.5$ F_2f initial levels. The cross sections were computed as a function of the collision energy, in order to allow calculation of the corresponding state-to-state rate constants.

Figure 5 presents energy dependent $K = 0$ and 1 tensor cross sections for several of the strongest transitions ($|\Delta j| \leq 2$ to all fine-structure/Λ-doublet levels) out of the $j = 10.5$ F_2f initial level to F_2f and F_1e final levels. It can be seen in Figs. 5(a) and 5(c) that the $K = 0$ tensor cross sections for exoergic transitions are large at low collision energies and decrease with increasing collision energy. This behavior is similar to that which was found[27] for the CN($A^2\Pi$)–Ar elastic depolarization cross sections, although the dependence upon collision energy is larger for the elastic depolarization cross sections. It can be seen in Fig. 5(a) the endoergic cross sections (i.e., $\Delta j = +1$ and $+2$) rise rapidly from their respective energy thresholds.

The $K = 1$ tensor cross sections for fine-structure conserving transitions, displayed in Fig. 5(b), show a similar dependence upon the collision energy as the corresponding $K = 0$ tensor cross sections [Fig. 5(a)], and the magnitudes of the former and latter are somewhat similar. By contrast, the $K = 1$ tensor cross sections for fine-structure changing transitions [Fig. 5(d)] show a different behavior than the corresponding $K = 0$ tensor cross sections [Fig. 5(c)]. The $\Delta j = +1$ cross section has a similar dependence upon collision energy as the corresponding $K = 0$ cross section, although the magnitude of the $K = 1$ cross section is much less.

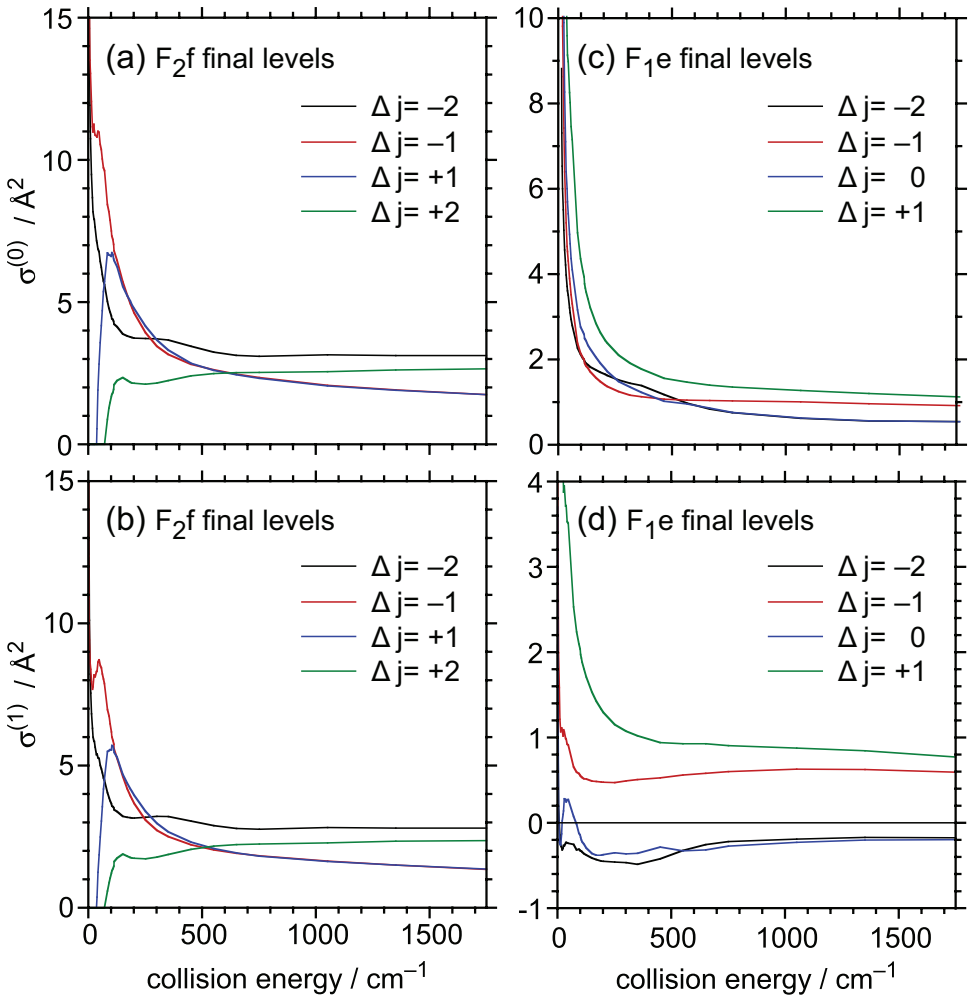

FIG. 5. Computed state-to-state tensor cross sections for transitions from the $j = 10.5$ F_2f initial level in collisions of CN($A^2\Pi$,v = 4) with Ar as a function of the collision energy. (a) $K = 0$ tensor cross sections to F_2f final levels, (b) $K = 1$ tensor cross sections to F_2f final levels, (c) $K = 0$ tensor cross sections to F_1e final levels, and (d) $K = 1$ tensor cross sections to F_1e final levels.

The $K = 1$ cross section for the $\Delta j = -1$ transition is fairly small and has a weak collision energy dependence. The $K = 1$ cross sections for even-Δj fine-structure changing transitions ($\Delta j = 0$ and -2) have a very different dependence upon collision energy and are predominantly negative. (Recall that the $K > 0$ tensor cross sections can be positive or negative.)

The state-to-state rate constants, $k^{(0)}_{j\rightarrow j'}$, and multipole transfer efficiencies, $E^{(1)}(j, j')$ [Eq. (9)], were calculated by thermally averaging the state-to-state tensor cross sections.[65] These computed quantities are plotted along with the experimental results in Figs. 3 and 4, respectively.

IV. DISCUSSION

A. Population transfer

We first briefly discuss the state-to-state population transfer results, $k^{(0)}_{j\rightarrow j'}$. Figures 3 and 4 in general show excellent agreement between experiment and theory in both overall magnitude and in the state-to-state propensities. There are, however, several discrepancies between experiment and theory. First, as shown in Fig. 3(a)(i), the experimentally determined cross sections for $\Delta j > 0$ from the $j = 6.5$ F_1e level are substantially larger than those predicted by theory. We believe this is partly due to an experimental artifact, the result of an accidental spectroscopic near-overlap in the pump step. The formation of the R-branch band head of the CN(A-X)(4,0) band results in the $R_1(5.5)$ and $R_1(10.5)$ transitions being separated by $\Delta\nu = 0.24$ cm^{-1}. Under the saturated pump conditions we have previously measured the effective full width at half maximum bandwidth of our pump laser to be $\Delta\nu \approx 0.5$ cm^{-1},[57,58] and hence when the pump laser was centered on the $R_1(5.5)$ transition some pump laser overlap with the $R_1(10.5)$ transition occurred, which resulted in the preparation of a small population in $j = 11.5$ F_1e. Population transfer from this initial level would be expected to be most probable into the $j' = 7.5$–9.5 F_1e product levels for which the largest experiment-theory disagreement is observed. Direct measurement of the $j = 11.5$ F_1e level indicated that the prepared population was typically ≈10% of that prepared in the desired $j = 6.5$ F_1e level. Under these conditions we expect that its contributions to any of the other observed product levels are likely to have been small compared to the reported experimental errors. In principle an attempt could have been made to subtract a weighted contribution of either experimental measurements or QS calculations originating from this

$j = 11.5\ F_1e$ level from the results presented in Fig. 3. However, substantial variations in the relative magnitudes of the population and orientation prepared in $j = 11.5\ F_1e$ are likely to have occurred from scan-to-scan, as a result of the accidental and un-optimised nature of the pump process. We therefore decided that separate measurements preparing a different initial state *via* an isolated transition, together with appropriate QS calculations, would provide more robust evidence of the scattering dynamics. The $P_2(11.5)$ transition used to prepare the $j = 10.5\ F_2f$ level is separated by >1 cm^{-1} from the nearest transition, and further isolated from transitions that terminate in levels energetically close to $j = 10.5\ F_2f$. We are therefore confident that excitation on this transition uniquely prepared $j = 10.5\ F_2f$.

Second, Figs. 4(a)(i) and 4(b)(i) show a small but systematic disagreement in the absolute magnitude of $k^{(0)}_{j\rightarrow j'}$ for transfer from $j = 10.5\ F_2f$. Here, theory predicts rate constants which are larger than experiment for nearly all of the observed product levels. This is consistent with the small (∼15%) systematic over-prediction of the total removal rate constants reported in our previous study and may result from a slight overestimate of the anisotropic range of the PESs.[27]

There are substantial alternations in the state-to-state rate constants $k^{(0)}_{j\rightarrow j'}$ with even/odd-Δj, which are superimposed on the commonly observed decrease of the rate constants with increasing $|\Delta j|$.[16] In Figs. 3(a)(i) and 4(a)(i) for the even-Δj spin-orbit and Λ-doublet conserving transitions the modulation depth is greater than observed for the odd-Δj spin-orbit and Λ-doublet conserving transitions. The converse is observed in Figs. 3(b)(i) and 4(b)(i) for the spin-orbit and Λ-doublet changing transitions, where odd Δj are favored.

These alternations reflect conservation of the parity: transfer between levels of the same parity is found to be more favourable than transfer that involves a change in parity. This effect has been previously observed, generally for collisions of molecules in $^2\Pi$ electronic states,[50] and more specifically in collisions of CN(A) RET with Ar and He.[73–75] The most comparable previous measurement is the relative state-to-state RET rate for relaxation of the adjacent vibrational level CN(A, v = 3) in collision with Ar, starting from the $j = 6.5\ F_1e$ level, with which we see excellent agreement.[56] As noted in the Introduction, collisions that conserve total parity can be shown to arise from the even-λ components in the angular expansion of the PESs, while those that change parity result from the odd-λ components.[48,49] The CN(A)-Ar PESs are dominated by even-λ terms in the angular expansions [Eqs. (2a) and (2b)],[27,55] often described as being "near homonuclear." This results in a strong propensity for conservation of the parity and hence the observed strong even/odd $k^{(0)}_{j\rightarrow j'}$ alternations. The good agreement between theory and experiment here is therefore strong evidence that the PESs accurately reproduce the even/odd nature of the CN(A) + Ar interaction.

B. Orientation transfer

We now turn to the main focus of this paper, the state-to-state transfer of rotational orientation, as measured by the multipole transfer efficiency (MTE), $E^{(1)}(j, j')$. We remind the reader that this quantity ranges between −1 and +1, where +1 represents complete conservation of the orientation of the initial level, zero represents net-zero product orientation, and −1 represents conservation in magnitude but reversal of the sign of the orientation in the product relative to that in the initial level.

Figures 3 and 4 show excellent agreement between experiment and theory in both the qualitative trends and the quantitative values of the MTEs. Broadly similar behavior is seen for both the $j = 6.5\ F_1e$ and $j = 10.5\ F_2f$ initial levels, confirming that the observations are a general feature of the CN(A) + Ar scattering dynamics. In each case, the MTEs show stronger conservation of initial orientation for spin-orbit conserving, compared to spin-orbit changing, transitions, with this propensity being more pronounced for the $j = 10.5\ F_2f$ initial level. However, the most striking observation is the strong oscillations in the state-to-state MTEs as a function of Δj, which on closer examination are found to depend on whether or not *parity* has been conserved, similar to the alternation in the state-to-state rate constants discussed in Sec. IV A.

In general, transfer that conserves the parity also tends to conserve the initially prepared orientation and results in positive MTEs, although these are generally less than unity, reflecting some depolarization. In contrast, transfer that results in a change in parity generally results in MTEs that are substantially smaller in magnitude, or as shown in Fig. 3(b)(ii), even *negative*. We reiterate the unexpectedness of this observation: Single collisions in an isotropic environment of a sample prepared with an initial laboratory-frame sense of rotation are found to result in product levels that for specific combinations of the initial and final levels rotate with the opposite laboratory-frame sense of rotation! These results hence suggest that the parity dependent oscillations in the MTE of the type observed by Norman and Field,[52] for a very restricted range of initial and final levels in CaF($A^2\Pi$) + Ar, may be a more general feature of $^2\Pi$ + Rg collisions.

This excellent agreement between the QS calculations and the experimental results encourages us to look at the calculations in more depth. Figures 5(a) and 5(b) show the $K = 0$ and $K = 1$ tensor cross sections for parity-conserving and changing transitions to a range of spin-orbit conserving product levels from the $j = 10.5\ F_2f$ initial level, as a function of the collision energy. The collision energy dependences of the respective $K = 0$ and $K = 1$ cross sections for a given spin-orbit conserving transition are very similar in form, although the absolute magnitudes of the $K = 1$ cross sections are slightly smaller. This implies a MTE that is largely constant (and near unity) as a function of collision energy for these transitions, and that does not vary greatly with the parity of the final level, consistent with the thermally averaged MTEs for these transitions shown in Fig. 4. In contrast, much larger differences in the relative $K = 0$ and $K = 1$ cross sections for different product levels are observed in Figs. 5(c) and 5(d), when spin-orbit changing transitions are considered. Here, for parity-conserving final levels, the collision energy dependences of the cross sections for $K = 0$ and $K = 1$ have very similar shapes, albeit with a substantially smaller magnitude for $K = 1$. Most strikingly, however, completely different

forms for the $K = 0$ and $K = 1$ cross sections are observed for the parity-changing final levels (even-Δj). The $K = 1$ cross sections for these collisions are nearly constant and negative for most of the range of collision energy, implying that their MTEs are negative and largely independent of collision energy beyond a limited range of energies that lie below the average in a thermal sample.

The energy dependence of these spin-orbit and parity-changing cross sections show no particular evidence that the observed change in the sign of the orientation arises from any particular collision energy range, for example, orbiting or trapping collisions within the attractive region of the PESs. Instead the orientation-changing behavior is relatively independent of collision energy for each particular product level. There are significant differences between the spin-orbit conserving and changing transitions. Because CN(A) is relatively close to the Hund's case (a) limit for these values of j, the spin-orbit conserving and changing collisions will be dominated by the $V_{\rm sum}$ and $V_{\rm dif}$ PESs, respectively.[49] Since the parity-conserving and parity-changing transitions result predominantly from the even and odd λ terms in the PES angular expansions respectively, this must be the result of the difference in this even/odd character between $V_{\rm sum}$ and $V_{\rm dif}$. Notably, the $V_{\rm dif}$ PES has a more even-λ character than the $V_{\rm sum}$, as by symmetry it lacks the lowest-order odd λ term in the angular expansions.

The dramatic change in the sign of the orientation for a molecule rotating initially in $j = 10.5$ requires a large transfer of angular momentum during the collision. An obvious question is whether the parity-conserving and parity-changing transfer arises from collisions at different impact parameters. For example, might we see large-impact-parameter "glancing" collisions that preserve polarization for the parity-conserving transitions, versus low-impact parameter "hard" collisions that change polarization for the parity-changing transitions? Figure 6(a) shows the computed $K = 0$ and $K = 1$ partial tensor opacity functions [cross sections as a function of the total angular momentum J, defined in Eq. (24) of Ref. 19], for transfer from $j = 10.5\ F_2f$ to $j' = 10.5\ F_1e$ and $j' = 9.5\ F_1e$, which are parity-changing and parity-conserving transitions, respectively, at a collision-energy of 300 cm^{-1}.

Substantial differences are apparent between the $K = 0$ and $K = 1$ partial tensor cross sections for both of these transitions. A high-J peak ($j = 70$–80) is observed in the $K = 0$ cross section for the parity-conserving transition that is absent for the parity-changing transition. Conversely, the parity-changing transition clearly has a larger $K = 0$ cross section across the lower-J range ($j = 0$–50). The parity-changing transitions are therefore on average influenced by collisions at lower impact parameter than the parity-conserving transitions. However, the $K = 1$ partial cross sections show that it is not simply this different range of contributing impact parameters that is the cause of the observed orientation alternation. The $K = 1$ cross section for the parity-conserving collisions is positive for all J, while the corresponding cross section for the parity-changing collisions is negative across almost the entire range of J. This is clearly shown in Fig. 6(b), where the MTE [the ratio of the relevant cross sections in Fig. 6(a)] is plotted as a function of J for the two transitions. Across the ranges

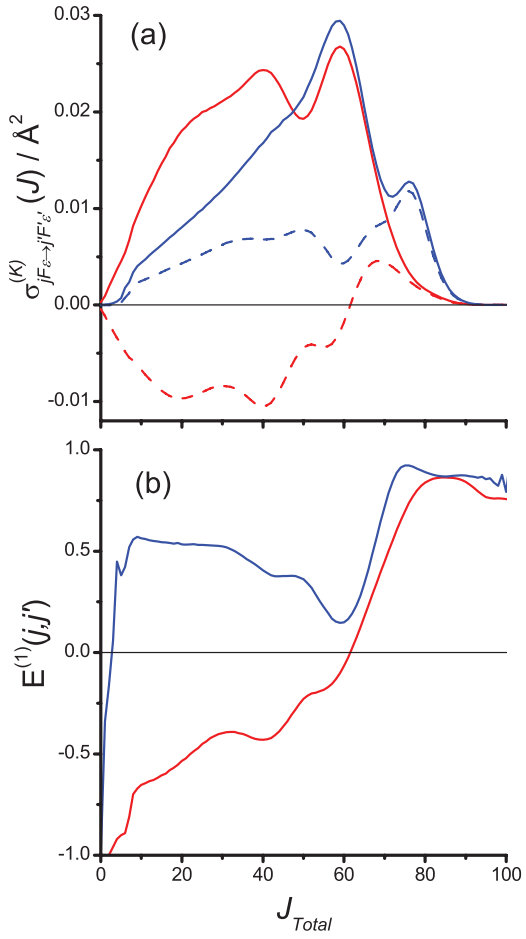

FIG. 6. (a) Computed tensor state-to-state partial cross sections for transitions from the $j = 10.5\ F_2f$ initial level in collisions of CN($A^2\Pi$,v = 4) with Ar at 300 cm^{-1} collision energy, for $K = 0$ (solid line) and $K = 1$ (dashed line) to product levels $j' = 10.5\ F_1e$ (red) and $j' = 9.5\ F_1e$ (blue). (b) Resulting partial multipole transfer efficiencies, $E^{(1)}(j, j')$, from $j = 10.5\ F_2f$ to $j' = 10.5\ F_1e$ (red) and $j' = 9.5\ F_1e$ (blue).

of J that contribute significantly for each transition, the MTE for the parity-conserving transition is positive, while the MTE for the parity-changing transition is almost always negative. Even at $J = 50$, which corresponds to a classical impact parameter of 3 Å, near the attractive minimum of the V_{sum} PES, the $K = 0$ partial cross sections are essentially identical, but the partial MTEs are still opposite in sign. The partial cross sections here clearly show that the dynamics of the collisions that lead to parity-conserving and parity-changing transitions are fundamentally different for reasons other than their opacity functions alone.

How can we explain this observation that different dynamics characterizes the scattering into levels of different final rotational parity? Presumably the answer must lie in the fact that different terms of the angular expansions of the PESs couple parity-conserving as compared with parity-changing transitions. The most relevant recent work is the combined experimental and theoretical investigation of Aoiz, Brouard, Stolte, and co-workers on NO($X^2\Pi$) + Ar/He.[3,6–8,76–81] They measured state-to-state differential cross sections (DCS) for RET with full initial and final-state resolution, including rotational parity, subsequent to collisions of a selected single

initial Λ-doublet level of the lowest $j = 0.5$ F_1 rotational level. Strong parity-dependent effects were observed in the DCS, with markedly different angular distributions observed for final levels of the same j' but different parity. QS calculations agree quantitatively with the experimental results. Detailed examination of the calculations shows that scattering from the same range of J gives rise to different DCSs for the levels of different final parity.[7]

Parity-dependent effects observed in NO($X^2\Pi$)–Rg DCS measurements may be reproduced not only by QS calculations but also explained qualitatively by the semi-classical Quasi-Quantum-Treatment (QQT) introduced by Stolte and co-workers.[3,77] This model approximates the scattering by classical rigid ellipse-rigid sphere kinematics, but allows for interference between paths which correspond to impacts at different points on the ellipsoidal surface but result in the same final rotational state and the same scattering. Stolte and co-workers identified different interfering trajectories as contributing to parity-changing versus parity conserving transitions.

It is possible that the origin of the newly observed oscillation in the MTEs for CN(A)-Ar arises from similar interference effects, despite the differences in the nature of the observables in the NO(X) crossed-beam experiments and those investigated here. It would be worthwhile to pursue application of the QQT (or similar) model to gain further insight into the MTE behavior observed here.

V. CONCLUSIONS

We have presented here the first systematic measurements of the efficiency of the transfer of a prepared rotational angular momentum orientation in state-to-state RET for a $^2\Pi$ + Rg system. We observed very strong state-to-state variations in the product orientation, including changes in sense of rotation. The accompanying QS calculations reproduce the experimental observations with near-quantitative agreement. This oscillation corresponds to a strong propensity to conserve orientation in rotational-parity conserving collisions, and a corresponding propensity to change orientation in parity-changing collisions. We suggest that this is a fundamental property of $^2\Pi$ − Rg collisions, and is closely related to the previously reported parity-dependent oscillations in the DCSs for other related $^2\Pi$ − Rg systems.

ACKNOWLEDGMENTS

S.J.McG thanks the Engineering and Physical Sciences Research Council for a Doctoral Training Award studentship for the experimental section of this work. M.H.A. and P.J.D. are grateful for support for the theoretical portion of this work from the U. S. National Science Foundation (Grant No. CHE-1213322).

[1]P. J. Dagdigian, in *Chemical Dynamics and Kinetics of Small Free Radicals*, edited by K. Liu and A. Wagner (World Science, Singapore, 1995), p. 315.
[2]M. L. Costen, S. Marinakis, and K. G. McKendrick, Chem. Soc. Rev. **37**, 732 (2008).
[3]A. Gijsbertsen, H. Linnartz, G. Rus, A. E. Wiskerke, S. Stolte, D. W. Chandler, and J. Kłos, J. Chem. Phys. **123**, 224305 (2005).
[4]E. A. Wade, K. T. Lorenz, D. W. Chandler, J. W. Barr, G. L. Barnes, and J. I. Cline, Chem. Phys. **301**, 261 (2004).
[5]K. T. Lorenz, D. W. Chandler, J. W. Barr, W. W. Chen, G. L. Barnes, and J. I. Cline, Science **293**, 2063 (2001).
[6]C. J. Eyles, M. Brouard, H. Chadwick, B. Hornung, B. Nichols, C. H. Yang, J. Kłos, F. J. Aoiz, A. Gijsbertsen, A. E. Wiskerke, and S. Stolte, Phys. Chem. Chem. Phys. **14**, 5403 (2012).
[7]C. J. Eyles, M. Brouard, H. Chadwick, F. J. Aoiz, J. Kłos, A. Gijsbertsen, X. Zhang, and S. Stolte, Phys. Chem. Chem. Phys. **14**, 5420 (2012).
[8]C. J. Eyles, M. Brouard, C. H. Yang, J. Kłos, F. J. Aoiz, A. Gijsbertsen, A. E. Wiskerke, and S. Stolte, Nat. Chem. **3**, 597 (2011).
[9]J. J. Kay, J. D. Steill, J. Kłos, G. Paterson, M. L. Costen, K. E. Strecker, K. G. McKendrick, M. H. Alexander, and D. W. Chandler, Mol. Phys. **110**, 1693 (2012).
[10]J. J. Kay, G. Paterson, M. L. Costen, K. E. Strecker, K. G. McKendrick, and D. W. Chandler, J. Chem. Phys. **134**, 091101 (2011).
[11]J. D. Steill, J. J. Kay, G. Paterson, T. R. Sharples, J. Kłos, M. L. Costen, K. E. Strecker, K. G. McKendrick, M. H. Alexander, and D. W. Chandler, J. Phys. Chem. A **117**, 8163 (2013).
[12]M. C. van Beek, G. Berden, H. L. Bethlem, and J. J. ter Meulen, Phys. Rev. Lett. **86**, 4001 (2001).
[13]G. Sarma, S. Marinakis, J. J. ter Meulen, D. H. Parker, and K. G. McKendrick, Nat. Chem. **4**, 985 (2012).
[14]L. Scharfenberg, J. Kłos, P. J. Dagdigian, M. H. Alexander, G. Meijer, and S. Y. T. van de Meerakker, Phys. Chem. Chem. Phys. **12**, 10660 (2010).
[15]J. J. Gilijamse, S. Hoekstra, S. Y. T. van de Meerakker, G. C. Groenenboom, and G. Meijer, Science **313**, 1617 (2006).
[16]A. Schiffman and D. W. Chandler, Int. Rev. Phys. Chem. **14**, 371 (1995).
[17]G. Paterson, M. L. Costen, and K. G. McKendrick, Mol. Phys. **109**, 2565 (2011).
[18]P. J. Dagdigian and M. H. Alexander, J. Chem. Phys. **130**, 094303 (2009).
[19]P. J. Dagdigian and M. H. Alexander, J. Chem. Phys. **130**, 164315 (2009).
[20]F. J. Aoiz, M. Brouard, C. J. Eyles, J. Kłos, and M. P. de Miranda, J. Chem. Phys. **130**, 044305 (2009).
[21]G. Paterson, S. Marinakis, J. Kłos, M. L. Costen, and K. G. McKendrick, Phys. Chem. Chem. Phys. **11**, 8804 (2009).
[22]G. Paterson, S. Marinakis, M. L. Costen, K. G. McKendrick, J. Kłos, and R. Toboła, J. Chem. Phys. **129**, 074304 (2008).
[23]S. Marinakis, G. Paterson, J. Kłos, M. L. Costen, and K. G. McKendrick, Phys. Chem. Chem. Phys. **9**, 4414 (2007).
[24]G. Paterson, S. Marinakis, M. L. Costen, and K. G. McKendrick, Phys. Chem. Chem. Phys. **11**, 8813 (2009).
[25]M. L. Costen, R. Livingstone, K. G. McKendrick, G. Paterson, M. Brouard, H. Chadwick, Y. P. Chang, C. J. Eyles, F. J. Aoiz, and J. Kłos, J. Phys. Chem. A **113**, 15156 (2009).
[26]G. Paterson, A. Relf, M. L. Costen, K. G. McKendrick, M. H. Alexander, and P. J. Dagdigian, J. Chem. Phys. **135**, 234304 (2011).
[27]S. J. McGurk, K. G. McKendrick, M. L. Costen, D. I. G. Bennett, J. Kłos, M. H. Alexander, and P. J. Dagdigian, J. Chem. Phys. **136**, 164306 (2012).
[28]I. Ballingall, M. F. Rutherford, K. G. McKendrick, and M. L. Costen, Mol. Phys. **108**, 847 (2010).
[29]S. R. Jeyes, A. J. McCaffery, and M. D. Rowe, Mol. Phys. **36**, 845 (1978).
[30]S. R. Jeyes, A. J. McCaffery, and M. D. Rowe, Mol. Phys. **36**, 1865 (1978).
[31]A. J. McCaffery, S. R. Jeyes, M. D. Rowe, and H. Kato, Ber. Bunsenges. Phys. Chem. **81**, 225 (1977).
[32]M. D. Rowe and A. J. McCaffery, Chem. Phys. **43**, 35 (1979).
[33]S. J. Silvers, R. A. Gottscho, and R. W. Field, J. Chem. Phys. **74**, 6000 (1981).
[34]G. O. Sitz and R. L. Farrow, J. Chem. Phys. **101**, 4682 (1994).
[35]A. D. Rudert, J. Martin, W. B. Gao, J. B. Halpern, and H. Zacharias, J. Chem. Phys. **111**, 9549 (1999).
[36]C. M. Wolfe, S. Ashman, J. Bai, B. Beser, E. H. Ahmed, A. M. Lyyra, and J. Huennekens, J. Chem. Phys. **134**, 174301 (2011).
[37]P. H. Vaccaro, F. Temps, S. Halle, J. L. Kinsey, and R. W. Field, J. Chem. Phys. **88**, 4819 (1988).
[38]S. L. Coy, S. D. Halle, J. L. Kinsey, and R. W. Field, J. Mol. Spectrosc. **153**, 340 (1992).
[39]V. Khare, D. J. Kouri, and D. K. Hoffman, J. Chem. Phys. **74**, 2275 (1981).
[40]M. H. Alexander and S. L. Davis, J. Chem. Phys. **78**, 6754 (1983).
[41]H. Chadwick, M. Brouard, Y. P. Chang, C. J. Eyles, T. Perkins, S. A. Seamons, J. Kłos, M. H. Alexander, and F. J. Aoiz, J. Chem. Phys. **137**, 154305 (2012).

[42]M. Brouard, H. Chadwick, Y. P. Chang, C. J. Eyles, F. J. Aoiz, and J. Kłos, J. Chem. Phys. **135**, 084306 (2011).
[43]M. Brouard, H. Chadwick, Y. P. Chang, R. Cireasa, C. J. Eyles, A. O. La Via, N. Screen, F. J. Aoiz, and J. Kłos, J. Chem. Phys. **131**, 104307 (2009).
[44]M. Brouard, A. Bryant, Y. P. Chang, R. Cireasa, C. J. Eyles, A. M. Green, S. Marinakis, F. J. Aoiz, and J. Kłos, J. Chem. Phys. **130**, 044306 (2009).
[45]M. Brouard, A. Bryant, I. Burak, S. Marinakis, F. Quadrini, I. A. Garcia, and C. Vallance, Mol. Phys. **103**, 1693 (2005).
[46]M. H. Alexander, Chem. Phys. **92**, 337 (1985).
[47]J. M. Brown, J. T. Hougen, K. P. Huber, J. W. C. Johns, I. Kopp, H. Lefebvrebrion, A. J. Merer, D. A. Ramsay, J. Rostas, and R. N. Zare, J. Mol. Spectrosc. **55**, 500 (1975).
[48]M. H. Alexander, J. Chem. Phys. **76**, 5974 (1982).
[49]P. J. Dagdigian, M. H. Alexander, and K. Liu, J. Chem. Phys. **91**, 839 (1989).
[50]C. Dufour, B. Pinchemel, M. Douay, J. Schamps, and M. H. Alexander, Chem. Phys. **98**, 315 (1985).
[51]M. H. Alexander and T. Orlikowski, J. Chem. Phys. **80**, 1506 (1984).
[52]J. B. Norman and R. W. Field, J. Chem. Phys. **92**, 76 (1990).
[53]M. H. Alexander and S. L. Davis, J. Chem. Phys. **79**, 227 (1983).
[54]X. Yang and P. J. Dagdigian, Chem. Phys. Lett. **297**, 506 (1998).
[55]M. H. Alexander, X. Yang, P. J. Dagdigian, A. Berning, and H. J. Werner, J. Chem. Phys. **112**, 781 (2000).
[56]X. Yang, P. J. Dagdigian, and M. H. Alexander, J. Chem. Phys. **112**, 4474 (2000).
[57]A. Alagappan, I. Ballingall, M. L. Costen, K. G. McKendrick, and G. Paterson, Phys. Chem. Chem. Phys. **9**, 747 (2007).
[58]A. Alagappan, I. Ballingall, M. L. Costen, and K. G. McKendrick, J. Chem. Phys. **126**, 041103 (2007).
[59]A. Alagappan, M. L. Costen, and K. G. McKendrick, Spectrochim. Acta A **63**, 910 (2006).
[60]S. Marinakis, G. Paterson, G. Richmond, M. Rockingham, M. L. Costen, and K. G. McKendrick, J. Chem. Phys. **128**, 021101 (2008).
[61]M. L. Costen, S. W. North, and G. E. Hall, J. Chem. Phys. **111**, 6735 (1999).
[62]I. Nadler, D. Mahgerefteh, H. Reisler, and C. Wittig, J. Chem. Phys. **82**, 3885 (1985).
[63]HIBRIDON is a package of programs for the time-independent quantum treatment of inelastic collisions and photodissociation written by M. H. Alexander, D. E. Manolopoulos, H.-J. Werner, B. Follmeg, and P. J. Dagdigian, with contributions by D. Lemoine, P. Vohralik, G. Corey, B. Johnson, T. Orlikowski, A. Berning, A. Degli-Esposti, C. Rist, B. Pouilly, J. Kłos, Q. Ma, G. van der Sanden, M. Yang, F. de Weerd, S. Gregurick, and F. Lique, see http://www2.chem.umd.edu/groups/alexander/hibridon/hib43.
[64]R. N. Zare, *Angular Momentum* (Wiley, New York, 1988).
[65]J. I. Steinfeld, J. S. Francisco, and W. L. Hase, *Chemical Kinetics and Dynamics* (Prentice Hall, Upper Saddle River, NJ, 1998).
[66]U. Fano and J. H. Macek, Rev. Mod. Phys. **45**, 553 (1973).
[67]K. Blum, *Density Matrix Theory and Applications*, 2nd ed. (Plenum Press, New York, 1996).
[68]A. J. Orr-Ewing and R. N. Zare, Annu. Rev. Phys. Chem. **45**, 315 (1994).
[69]R. Uberna, R. D. Hinchliffe, and J. I. Cline, J. Chem. Phys. **103**, 7934 (1995).
[70]M. L. Costen and G. E. Hall, Phys. Chem. Chem. Phys. **9**, 272 (2007).
[71]S. W. North, X. S. Zheng, R. Fei, and G. E. Hall, J. Chem. Phys. **104**, 2129 (1996).
[72]H. Meyer and S. R. Leone, J. Chem. Phys. **105**, 5858 (1996).
[73]N. Furio, A. Ali, and P. J. Dagdigian, J. Chem. Phys. **85**, 3860 (1986).
[74]G. Jihua, A. Ali, and P. J. Dagdigian, J. Chem. Phys. **85**, 7098 (1986).
[75]B. Nizamov, P. J. Dagdigian, and M. H. Alexander, J. Chem. Phys. **115**, 8393 (2001).
[76]A. Gijsbertsen, H. Linnartz, and S. Stolte, J. Chem. Phys. **125**, 133112 (2006).
[77]A. Gijsbertsen, H. Linnartz, C. A. Taatjes, and S. Stolte, J. Am. Chem. Soc. **128**, 8777 (2006).
[78]J. Kłos, F. J. Aoiz, J. E. Verdasco, M. Brouard, S. Marinakis, and S. Stolte, J. Chem. Phys. **127**, 031102 (2007).
[79]F. J. Aoiz, J. E. Verdasco, M. Brouard, J. Kłos, S. Marinakis, and S. Stolte, J. Phys. Chem. A. **113**, 14636 (2009).
[80]M. Brouard, H. Chadwick, C. J. Eyles, B. Hornung, B. Nichols, F. J. Aoiz, P. G. Jambrina, S. Stolte, and M. P. de Miranda, J. Chem. Phys. **138**, 104309 (2013).
[81]M. Brouard, H. Chadwick, C. J. Eyles, B. Hornung, B. Nichols, F. J. Aoiz, P. G. Jambrina, and S. Stolte, J. Chem. Phys. **138**, 104310 (2013).